Proceedings of 2nd International Conference on Climate Change and Emerging Trends in Civil Engineering CCETC-2025

Numerical Study on Moment Redistribution in Continuous Concrete Beams Reinforced with FRP Bars

Muhammad Saad Ifrahim[1*], Abdul Jabbar Sangi[1], Rajesh Kumar[1] and Muhammad Owais[1]

[1] Department of Civil Engineering, NED-UET, Sindh, Pakistan; msaadifrahim@cloud.neduet.edu.pk; ajsangi@cloud.neduet.edu.pk; rajeshkumarlohana97@gmail.com; owaismunir246@gmail.com
*Correspondence: msaadifrahim@cloud.neduet.edu.pk

Abstract

In harsh environments, steel rebars in concrete corrode; therefore, fiber-reinforced polymer (FRP) bars should be considered due to their non-corrosive nature. Moment distribution in continuous FRP-reinforced concrete beams is prohibited by the design code due to the insufficient ductility of FRP bars. However, studies have shown that FRP-reinforced concrete continuous beams exhibit considerable redistribution of moment. In this study, a nonlinear finite element model of a continuous concrete beam reinforced with basalt FRP bars is developed to numerically investigate the effect of reinforcement configuration on the redistribution of moment. The models exhibit a considerable level of moment redistribution at the internal support (hogging zone) and midspan (sagging zone). When the amount of tensile reinforcement in the sagging zone increases compared to the hogging zone, the moment redistribution at the internal support (hogging zone) increases significantly. Therefore, it is not justified to completely overlook the redistribution of moment in the design of FRP RC continuous beams.

Keywords: Moment Redistribution, Continuous Beam, Reinforced Concrete, Basalt Fiber Reinforced Polymer (BFRP)

1. Introduction

In harsh environments, like the coastal areas of Karachi and Gwadar, steel rebars in reinforced concrete get corroded due to saline water ingress. Corrosion reduces the cross-sectional area of rebars, which results in lower load-carrying capacity that might cause premature failure of RC members. According to [1,2], when steel reinforcement gets corroded, it suffers a considerable reduction in yield/ultimate strength and ductility. Therefore, it is imperative to find solutions to this grave problem. A possible solution is to use non-corrosive reinforcement in members that are subjected to hostile environments. Fiber reinforced polymer (FRP) bars can be used as a possible replacement for traditional steel owing to their non-corrosive nature [3]. Also, these bars offer high tensile strength, lower density, and non-magnetic properties [4]. There are many different types of FRP bars available in the market made from different fibers, including Glass, Carbon, Aramid, and Basalt. Among them, Basalt FRP bars are the most sustainable due to the need for less energy in production compared to others. [5]

FRP bars can be effectively used as flexural and shear reinforcement based on several studies [6–9]. They fail either due to concrete crushing or rupture of the bar. The linearly elastic behavior of FRP bars raises concerns about the ductility of FRP reinforced concrete members. The moment redistribution in FRP RC members is overlooked due to the lack of ductility in these bars. Until now, in the design code, moment redistribution is not allowed in FRP reinforced concrete

 https://doi.org/10.64615/fjes.1.Special Issue.2025.47

continuous beams [10]. However, in the recent decade, several researches have highlighted that ignoring moment redistribution in FRP RC members is not justified. According to the experiments conducted by Mahmoud and El-Salakaway [11], moment redistribution at the hogging region is either equal to or more than 20%. In another study by the same authors [12], it was found that continuous beams reinforced with GFRP bars exhibit a considerable level of moment redistribution at internal support before failing in shear. Santos et al. [13] carried out a study to investigate moment redistribution in two-span GFRP RC beams with different reinforcement arrangements. It was found that the reinforcement arrangement significantly influenced moment redistribution, as at the internal support, up to 63.7% moment redistribution was observed against a particular reinforcement arrangement. Shamass et al. [14] conducted a study on two span continious concrete beams reinforced with BFRP bars and concluded that BFRP RC beams exhibited at least 20% moment redistribution. Recently, Lou et al. [15] also reported that depending on how the reinforcement is arranged, FRP RC beams may undergo a positive or negative redistribution of moments.

These findings indicate that while progress has been made in understanding moment redistribution in FRP reinforced concrete, further research is necessary to fully comprehend the mechanisms involved and to develop comprehensive design guidelines. Therefore, this study investigates moment redistribution in BFRP reinforced concrete two-span continuous beams using a nonlinear finite element model on ATENA 2D. The study mainly examines how changing the ratio of tensile reinforcement in the sagging zone (ρ_{r1}) to the hogging zone (ρ_{r2}) affects moment redistribution in both regions.

2. Methodology

Shamass et al. [14] experimentally investigated continuous concrete beams reinforced with BFRP bars. The beams were designed according to ACI 440 guidelines for FRP bars in RC structures [10]. The beam's length was 4200 mm, and its cross-section was 200 mm (width) by 270 mm (depth), as shown in Fig. 1. A nonlinear Finite Element model was developed for one of the beams (B-0.24-0.24) tested by Shamass et al. [14] using ATENA 2D. The model comprises six macro elements: a beam specimen, loading plates, and supports. Fig. 2 shows the model with its boundary conditions: the first support is restrained in both the horizontal and vertical directions, while the middle and last supports are restricted to the vertical direction only. The bottom fiber of the sections where the loads are applied has a monitoring point for capturing deflection. The longitudinal bars are modelled using two node truss elements and 20 mm mesh size plane isoparametric quadrilateral elements (CCIsoQuad) are used. A thorough mesh sensitivity study is used to determine the mesh's size. In this FE model, SBETA material model is used for concrete (22.1 MPa) and a linearly elastic model for BFRP longitudinal bars and stirrups. The material properties of BFRP bars are given in Table 1. In Fig. 3, the Load deflection response shows that there is a good agreement between experimental results and numerical analysis; therefore, the developed FE model can be used for further numerical assessment.

Table 1. Material Properties of BFRP bars.

Type of bar	Bar diameter (mm)	Tensile Strength (MPa)	Elastic Modulus (GPa)
Main Bar	8.4	1018	44.5
Stirrup	8.4	1151	47.8

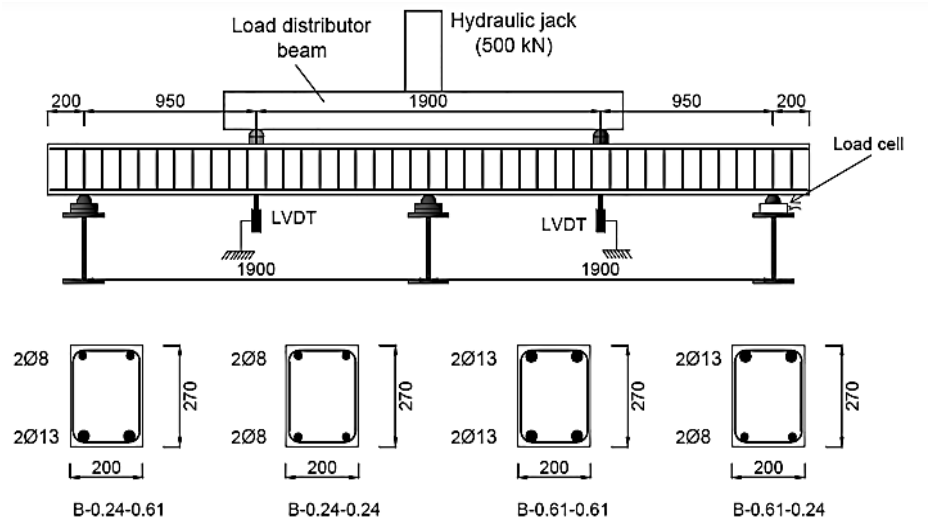

Figure 1. Experimental setup and tested beams. [14]

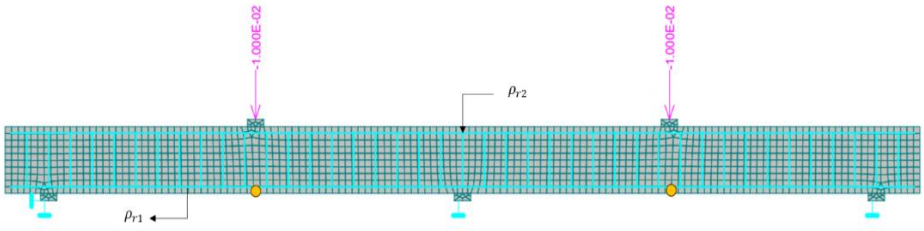

Figure 2. FE model of B-0.24-0.24.

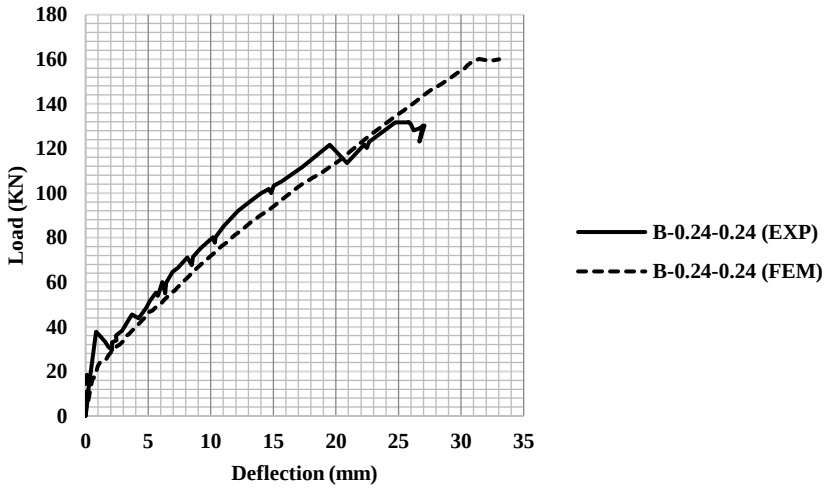

Figure 3. Load deflection response of B-0.24-0.24 from experimental study and numerical analysis.

3. Details of Numerical Models

This numerical study analyzes how changing the ratio of tensile reinforcement in the sagging zone to the hogging zone (ρ_{r1}/ρ_{r2}) affects the load-deflection response and moment redistribution in a continuous concrete beam reinforced with BFRP bars. Table 1 provides a test matrix that gives details of numerical models based on which numerical assessment is carried out.

Beams	fc' (MPa)	Flexural Reinforcement (BFRP)		Reinforcement ratio (%)		$\frac{\rho_{r1}}{\rho_{r2}}$	Stirrups (BFRP)	
		Bottom	Top	ρ_{r1}	ρ_{r2}		Bar size (mm)	Spacing (mm)
B-0.24-0.24	22.1	2 ϕ8.4	2 ϕ8.4	0.24	0.24	1	8.5	100
B-0.24-0.33	22.1	2 ϕ10	2 ϕ8.4	0.33	0.24	1.38	8.5	100
B-0.24-0.48	22.1	2 ϕ12	2 ϕ8.4	0.48	0.24	2	8.5	100
B-0.24-0.61	22.1	2 ϕ14	2 ϕ8.4	0.61	0.24	2.54	8.5	100
B-0.24-0.86	22.1	2 ϕ16	2 ϕ8.4	0.86	0.24	3.58	8.5	100

4. Results and Discussion

4.1. Load vs. Deflection Response

The load-deflection responses of the aforementioned numerical models are presented in Fig. 4. It shows the influence of increasing ρ_{r1}/ρ_{r2} on the overall global response of BFRP reinforced concrete continuous beam. It shows that with an increase in ρ_{r1}/ρ_{r2} ratio, there has been a significant improvement in stiffness since bottom reinforcement has increased. Fig. 5 (a) and 5 (b) show a fringe increment in load-carrying capacity and a significant decrease in deflection, respectively. When ρ_{r1}/ρ_{r2} increases from 1 to 3.58, there is an 18% increase in load carrying capacity while deflection, considering the load carrying capacity of B-0.24-0.24 as a baseline, has decreased by 63%. The considerable reduction in deflection due to increased stiffness is beneficial for the serviceability design criteria.

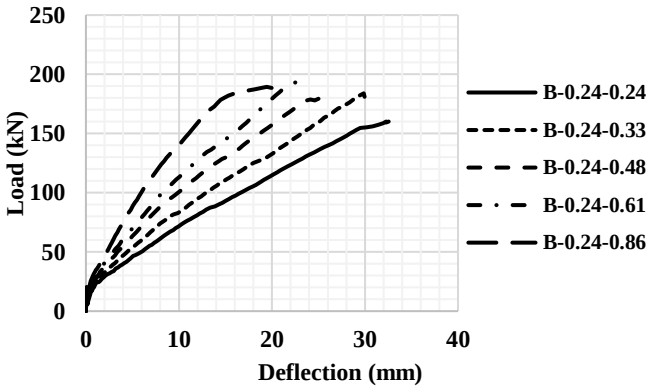

Figure 4. Effect of ρ_{r1}/ρ_{r2} on load-deflection response.

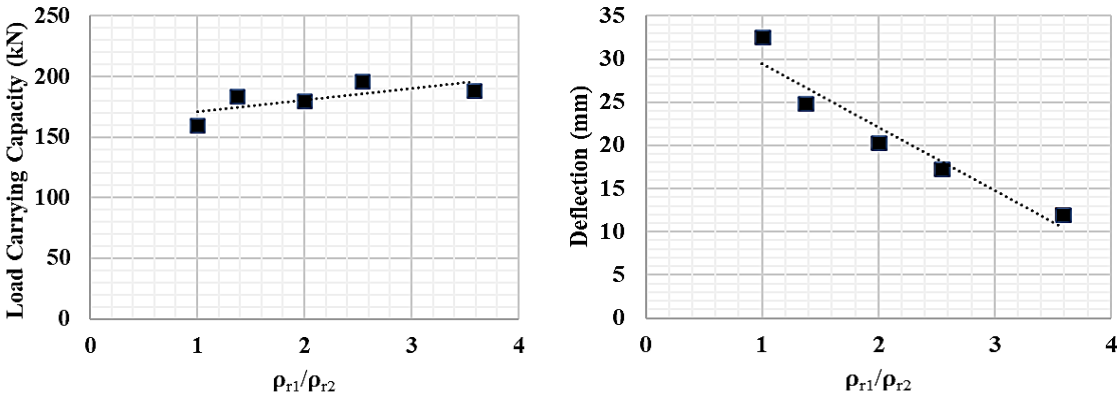

(**a**) (**b**)

Figure 5. Effect of ρ_{r1}/ρ_{r2} on (a) load-carrying capacity and (b) deflection corresponding to the load-carrying capacity of B-0.24-0.24.

4.2. Strain Profile

The strain profiles of all the numerical models with crack patterns are given in Fig. 6. It shows that an increase in ρ_{r1}/ρ_{r2}, the tensile strain in the mid-span section decreased significantly compared to the section at the center support. This is attributed to the considerable increase in stiffness at the mid-span section compared to the center support section with an increase in ρ_b/ρ_t. This facilitates the center support section in distributing the moment to the mid-span section. Additionally, it is observed that the compression-controlled failure mode governs all of the models.

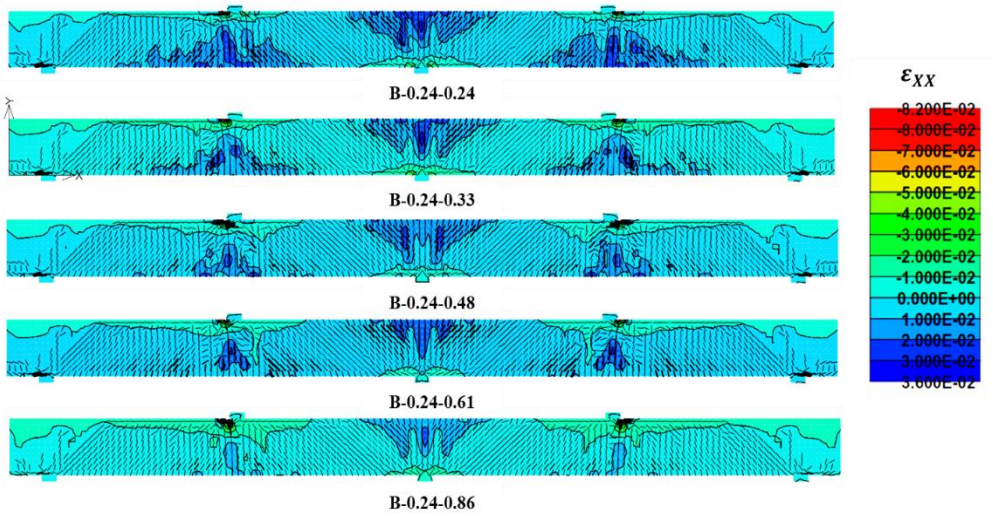

Figure 6. Strain profiles along with crack pattern at ultimate load.

4.3. Moment Redistribution

Fig. 7 shows moment diagrams of beams with different ρ_{r1}/ρ_{r2} ratios. The beam with $\rho_{r1}/\rho_{r2} = 1$ has a moment diagram closer to the elastic one at both the midspan section (sagging zone) and center support (hogging zone), which indicates there is marginal moment redistribution attributed to the same stiffness at both sections. However, when ρ_{r1}/ρ_{r2} is greater than 1, there is substantial moment redistribution at hogging and sagging zones attributed to increased stiffness at the mid-span section compared to the center support section due to increasing bottom reinforcement. At ultimate, the redistribution values of beams with $\rho_{r1}/\rho_{r2} = 1 - 3.58$ vary between -0.4% and -21% at midspan, while between 5.9% and 44.8% at center support. In Fig. 8, the trend of moment redistribution against increasing ρ_{r1}/ρ_{r2} is presented, which shows a good linear relationship between them, as the value of R^2 is greater than 0.9 for both midspan and center support sections.

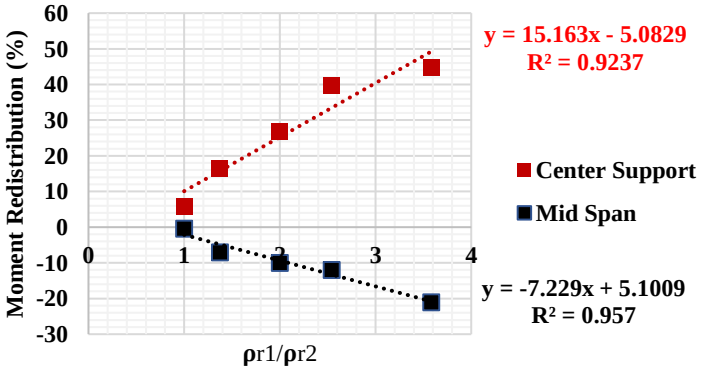

Figure 7. Effect of increasing ρ_{r1}/ρ_{r2} on moment redistribution at sagging and hogging zones.

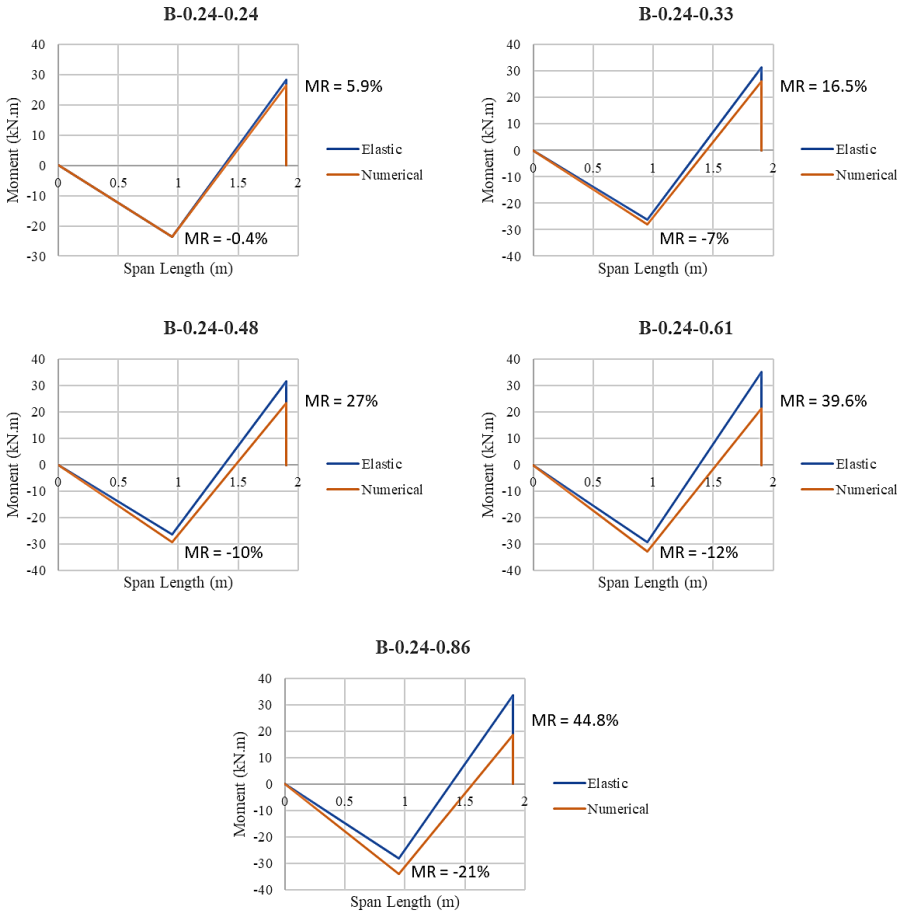

Figure 8. Moment diagrams at ultimate for beams with various ρ_{r1}/ρ_{r2}.

5. Conclusions

After detailed numerical analysis, the following conclusions are established:

1. There is a good agreement between the experimental results of Shamass et al. [14] and the developed Finite Element model in this comprehensive study.
2. It is found that the effect of increasing ρ_{r1}/ρ_{r2} in BFRP RC continuous beams on load carrying capacity is marginal. However, a substantial decrease in deflection has been observed which is beneficial from the point of view of serviceability.
3. BFRP RC continuous beams exhibit considerable moment redistribution; therefore, neglecting it in design is not justified. ACI 440 should reconsider the complete exclusion of moment redistribution in design equations, particularly for specific reinforcement configurations that promote redistribution as found in this study.
4. The ratio ρ_{r1}/ρ_{r2} is an critical factor that substantially affects the moment redistribution of BFRP reinforced concrete continuous beams. For example, the redistribution values of beams with $\rho_{r1}/\rho_{r2} = 1 - 3.58$ vary between -0.4% and -21% at midspan, while between 5.9% and 44.8% at center support.

Acknowledgments: The authors express their sincere gratitude to the Sindh Higher Education Commission for funding the ongoing research project through Sindh Research Support Program (SRSP/314/2023-24), and the Department of Civil Engineering, NED University of Engineering and Technology, Karachi, Pakistan, for their support and help.

Disclosure of Interests: Authors have no competing interests.

References

1. Apostolopoulos CA, Papadakis VG. Consequences of steel corrosion on the ductility properties of reinforcement bar. Constr Build Mater 2008;22:2316–24. https://doi.org/https://doi.org/10.1016/j.conbuildmat.2007.10.006.
2. Ožbolt J, Balabanić G, Kušter M. 3D Numerical modelling of steel corrosion in concrete structures. Corros Sci 2011;53:4166–77. https://doi.org/https://doi.org/10.1016/j.corsci.2011.08.026.
3. Nanni A, De Luca A, Jawaheri Zadeh H. Reinforced concrete with FRP bars mechanics and design 2014.
4. Lorenzis L De, Nanni A. An Introduction to FRP Composites for Construction. ACI Struct J 2002.
5. Ross A. Basalt fibers: alternative to glass? Compos Technol 2006;12.
6. Kara IF, Ashour AF. Flexural performance of FRP reinforced concrete beams. Compos Struct 2012;94:1616–25. https://doi.org/10.1016/j.compstruct.2011.12.012.
7. Saafi, Mohamed HA. Flexural Behavior of Concrete Beams Reinforced with Glass Fiber-Reinforced Polymer (GFRP) Bars. ACI Struct J 2000;97. https://doi.org/10.14359/8806.
8. Krall M, Polak MA. Concrete beams with different arrangements of GFRP flexural and shear reinforcement. Eng Struct 2019;198. https://doi.org/10.1016/j.engstruct.2019.109333.
9. Ifrahim MS, Sangi AJ, Ahmad SH. Experimental and numerical investigation of flexural behaviour of concrete beams reinforced with GFRP bars. Structures 2023;56:104951. https://doi.org/https://doi.org/10.1016/j.istruc.2023.104951.
10. ACI 440.1 R-15. Guide for the design and construction of structural concrete reinforced with FRP bars. Farmington Hills, MI: American Concrete Institute; 2015.
11. Karam M, Ehab E-S. Shear Strength of GFRP-Reinforced Concrete Continuous Beams with Minimum Transverse Reinforcement. J Compos Constr 2014;18:4013018. https://doi.org/10.1061/(ASCE)CC.1943-5614.0000406.
12. Karam M, Ehab E-S. Effect of Transverse Reinforcement Ratio on the Shear Strength of GFRP-RC Continuous Beams. J Compos Constr 2016;20:4015023. https://doi.org/10.1061/(ASCE)CC.1943-5614.0000583.
13. Santos P, Laranja G, França PM, Correia JR. Ductility and moment redistribution capacity of multi-span T-section concrete beams reinforced with GFRP bars. Constr Build Mater 2013;49:949–61. https://doi.org/https://doi.org/10.1016/j.conbuildmat.2013.01.014.
14. Shamass R, Mahi B, Cashell KA, Abarkan I, El-Khannoussi F. Experimental investigation into the behaviour of continuous concrete beams reinforced with basalt FRP. Eng Struct 2022;255:113888.
15. Lou T, Shi S, Lopes SMR, Chen B. Rational prediction of moment redistribution in continuous concrete beams reinforced with FRP bars. Eng Struct 2024;303:117515.